

Semiconductor TiO₂ Coating Deposited by Microwave Plasma Method

NOVRIANY Amaliyah^{1,a*}, AZWAR Hayat^{1,b}, ANDI ERWIN Eka Putra^{1,c}
ISMAIL Rahim^{2,d}, ASRIADI Sakka^{1,e}

¹Mechanical Engineering Department, Faculty of Engineering, Hasanuddin University
Gowa Kampus, Poros Malino Km. 6 Bontomarannu, Gowa, South Sulawesi, Indonesia 92171

²Automotive Technology Vocational Education Department, Faculty of Engineering, Universitas
Negeri Makassar. Mallengkeri Raya Parang Tambung, Makassar,
South Sulawesi, Indonesia 90224

^anovriany@unhas.ac.id, ^bazwar.hayat@unhas.ac.id, ^cerwinep@eng.unhas.ac.id,
^dismail_rahim@unm.ac.id, ^easriadisakka@unhas.ac.id

Keywords: Plasma, microwave, coating, titanium dioxide

Abstract. Transparent conducting glass is a crucial layer of Dye Synthesized Solar Cell (DSSC), due to it allows sunlight penetrating to the solar cell. DSSC has a low efficiency until semiconductor Titanium Dioxide (TiO₂) was employed as the anode material. TiO₂ has high photosensitivity, high structure, stability under solar irradiation and in solution, and low cost. In this study, TiO₂ was deposited on the conductive glass using microwave plasma method. Plasma was generated using electromagnetic waves from microwave magnetron. TiO₂ powder was dissolved using pure water and ethanol at different concentrations. The coating process was conducted on a 2.5 x 2.5 cm of conductive glass, and the effect of plasma generation time was observed at 0.5, 1, 2, 3, and 5 minutes. The thickness, roughness, and microstructure of TiO₂ coating on the conductive glass were observed using a 3D measuring laser OLS4100. The result shows that the fabrication of TiO₂ coatings using microwave plasma is feasible. The concentration of solution and plasma generation time plays an important role in the thickness, roughness, and microstructure of TiO₂ coatings. An optimum result was obtained at a plasma generation time of 0.5 minutes with 12.49 μm and 3.398 μm of thickness and roughness respectively using 10 g TiO₂ + 50 ml ethanol and 40 ml H₂O.

Introduction

Dye Synthesized Solar Cell (DSSC) has been extensively considered a promising photovoltaic device recently due to the low fabrication cost, optical properties, and high efficiency of power conversion [1, 2, 3]. It consists of a conductive glass substrate, a dye-synthesized metal oxide semiconductor electrode, a catalyst counter electrode, and an electrolyte solution inserted between the two electrodes. The conductive glass substrate should possess good electrical conductivity to provide a gateway for solar radiation to absorb also as a current collector [4].

There are some prominent metal oxides with band gaps higher than 3 eV that have good photo-corrosion resistance and superior electronic properties such as TiO₂, ZnO, SnO₂, SrTiO₃, Zn₂SnO₄, WO₃, and Nb₂O₅ to name a few [5]. TiO₂ is widely used as a semiconductor in DSSC due to high thermal, and chemical stability, low cost, favorable charge carrier properties, and high transparency in the solar spectrum [1]

The fabrication of TiO₂ nanoparticles on conductive glass plays an important role in the solar cells' efficiency since the thickness of the TiO₂ coating affects it. Various surface coating methods using TiO₂ were reported such as sol-gel [6], spray deposition [7], sequential dip spin[8], and chemical vapor deposition[9]. However, those methods often require high temperatures, multiple steps, and vacuum processing to produce a film.

The plasma method has been applied widely in nanoparticle production [10, 11]. This development has heightened the research on the plasma coating process. A plasma spray copper coating has been presented using two different plasma power of 20 kW and 25 kW. The result showed that 25 kW plasma power possesses higher density and hardness, advancing contact angle, and parahydrophobic

behavior that helps in better heat transfer at higher high flux [12]. The plasma electrolytic oxidation method successfully achieved high photocatalytic ability for the TiO₂ coating with a pulsed power mode in a range of 200 to 400 V using NaPO₃ as an alkaline electrolyte [13]. Atmospheric pressure plasma-enhanced chemical vapor deposition was applied to the TiO₂ coating on transparent plastic. An amorphous structure without any crack was successfully formed without damaging the polymer structure [14].

In this study, the feasibility of the TiO₂ coating using the microwave plasma method was investigated with various TiO₂ solutions and plasma irradiation time.

Experimental Procedure

The coating process of TiO₂ was conducted using a 2.45 GHz microwave plasma with an input power of 160 Volt. The electromagnetic wave from microwave magnetron was used to generate plasma. A transparent conductive glass 2.5 x 2.5 cm was hung inside a stainless steel reactor. Plasma was generated at the tip of the tungsten electrode with 2.5 cm space from the transparent conductive glass as shown in Fig. 1.

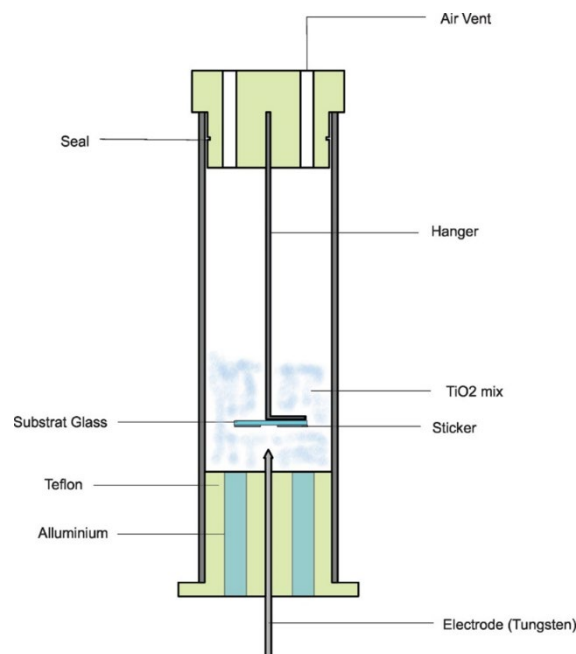


Fig. 1. Schematic illustration of TiO₂ coating by plasma

Table 1. Various concentrations of titanium dioxide solution

Solution	TiO ₂ powder (g)	Ethanol (ml)	Deionized water (ml)
I	5	100	40
II	10	100	40
III	20	100	40
IV	10	50	40

The solution was prepared by making various concentrations of titanium dioxide (TiO₂) with ethanol and pure water as shown in Table 1. A commercial non-branded Titanium Dioxide powder with a nominal particle size of 15 nm was used as a feedstock. The solution was then stirred for 2 h using a magnetic stirrer and poured inside the reactor, then plasma was generated within 2 minutes of irradiation time to compare the thickness and roughness of the coating result. The solution yields an optimum coating result then used to observe the effect of plasma irradiation time of 0.5, 1, 2, 3, and 5 minutes. The thickness, roughness, and microstructure of TiO₂ coating deposited on the conductive glass were then observed using a 3D measuring laser OLS4100.

Results and Discussion

TiO₂ Coating Results in Various Concentration of a Solution. Figures 2 and 3 shows a roughness measurement record and roughness average with a variation of solution after 2 min of plasma irradiation. The average roughness (Ra) is a coating surface roughness quantity that is defined as the arithmetic mean of departures of the profile from the mean line. The average roughness was 0.74 μm , 4.11 μm , 12.3 μm , and 3.67 μm for a solution I, II, III, and IV respectively.

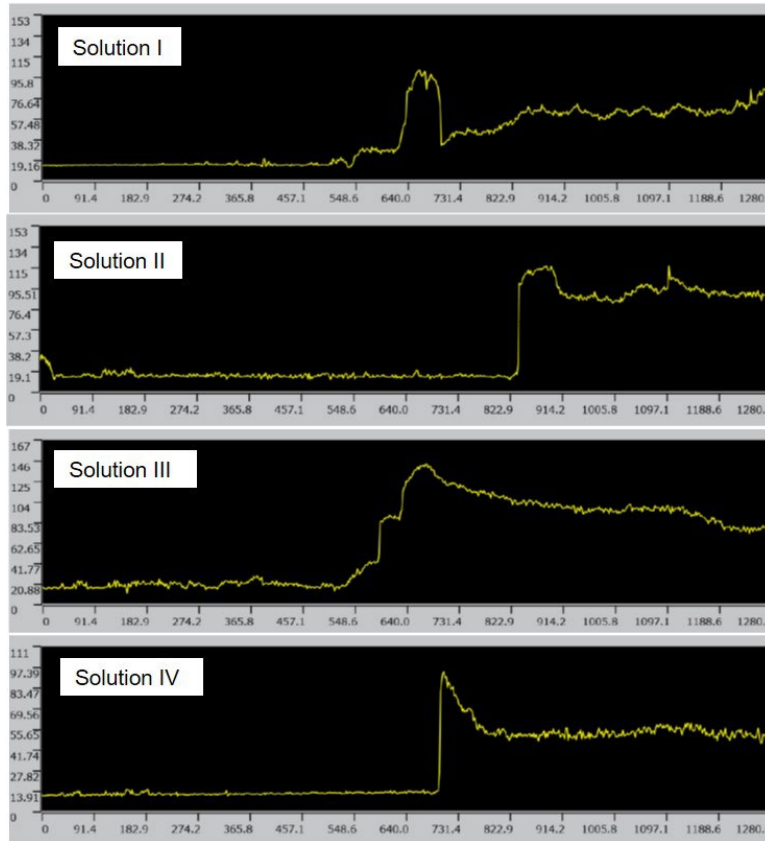


Fig. 2. Roughness measurement record of TiO₂ coating at various TiO₂ solution

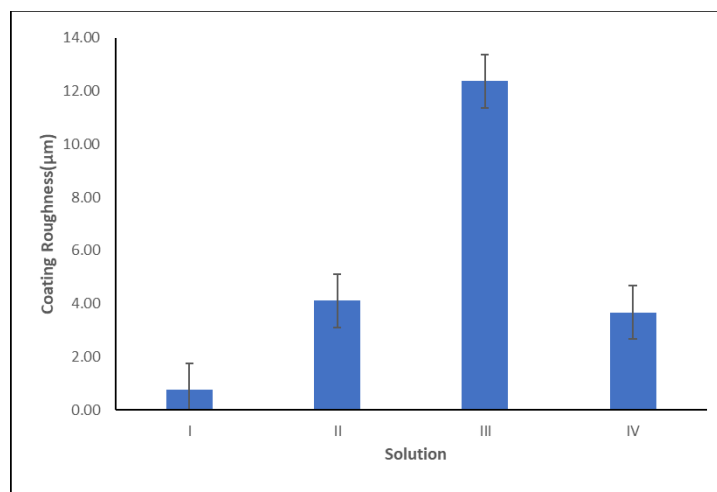


Fig. 3. Coating roughness average with a variation of TiO₂ solution

Increasing the amount of TiO₂ exhibits high roughness of the coating layer. The highest roughness was obtained when using solution III (20 g TiO₂ + 100 ml ethanol + 40 ml pure water). Following the present result, previous studies have demonstrated that the roughness of the coating surface was enhanced by increasing the particle concentration [15]. Research on micro-arc oxidation coupled with

electrophoretic deposition processing of HA/ TiO₂ coating indicated that the number of HA particles integrated into the coating layer increased as the HA concentration increased [16] When plasma electrolytic oxidation was applied to ceria nanocomposite coating and ZrO₂ nanoparticle on titanium substrate, it was reported that by increasing the concentration of nanoparticle the average size of surface roughness values was increased. It is assumed that they were not deposited in the pores but a few particles attached to the surface attributed to the increase of coating surface [17], [18]. However, when the amount of ethanol in the solution was decreased in solution IV (10 g TiO₂ + 50 ml ethanol + 40 ml pure water), the coating roughness decreased to 3.672 μm. Compared to other plasma coating methods, alumina coating by the air plasma spraying process reported the coating roughness in a range of 6.84 μm to 10.23 μm [15].

Figure 4 shows a coating thickness average with a variation of solution. Coating thickness was 58.03 μm, 64.91 μm, 84.18 μm, and 15.50 μm for a solution I, II, III, and IV, respectively. The same trend with coating roughness was also observed, the coating thickness was increased as the concentration of TiO₂ in solution I to III, then decrease when the amount of ethanol was decreased in solution IV. Although some researchers stated that adding particles into the electrolyte did not affect the thickness of the coating [19, 20, 21], in several papers, the increase in the coating thickness in exchange for the addition of concentration has been mentioned. Micro arc oxidation coatings with the addition of Al₂O₃ particles, MgO microparticles, and CeO₂-doped TiO₂ nanostructured composite revealed that the coating thickness result was increased. The finding from these studies indicates that the perceived increment in thickness might be related to the coating band gap declining, an increase in electrolyte conductivity, and the augmenting formation voltage of coating affected by increasing concentration [22, 23, 24].

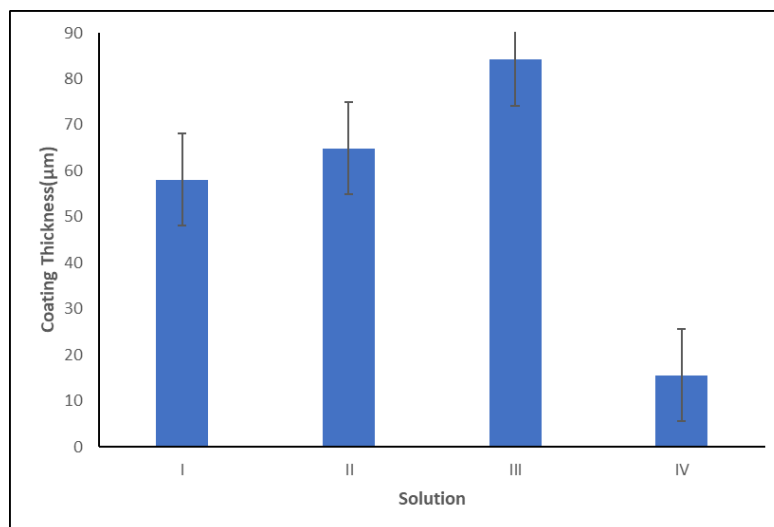


Fig. 4. Coating thickness average with a variation of TiO₂ solution

By varying the TiO₂ concentration, the optimum condition of thickness and roughness of 15.903 μm and 3.672 μm respectively was obtained using solution IV (10 g TiO₂ + 50 ml ethanol + 40 ml pure water). This solution was then used to observe the effect of plasma irradiation time.

The microstructure and 3D topography of TiO₂ coating with solution variation are shown in Figs. 5 and 6. Most coatings had the usual microstructure such as a porous surface with many micropores over the surface [15]. The formation of porous morphology was in consequence of molten materials left from the discharge channels and agglomerating around the opening due to the electric micro-discharge [25]. As can be seen in Fig. 5, increasing concentration resulting smaller pore and so does when the ethanol concentration decrease. In solution IV, pores with an average size of 7.42 μm were detected. A compact columnar structure was observed with similar morphology to other plasma coating methods [26, 14]. Coating of alumina nanoparticles on titanium substrate via plasma electrolytic oxidation also confirmed that increasing the concentration of nanoparticles promotes the

peak intensity and shifts the peak position to smaller pores with pores diameter in a range of 3 to 10 μm [20].

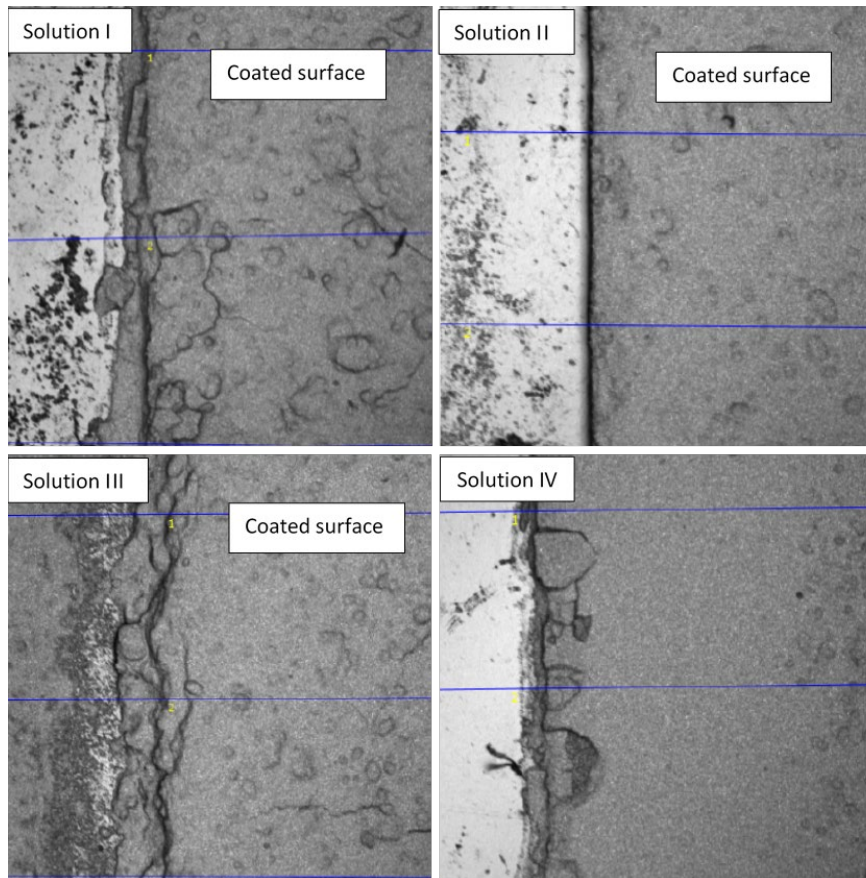


Fig. 5. Microstructure surface TiO_2 coating at various TiO_2 solution

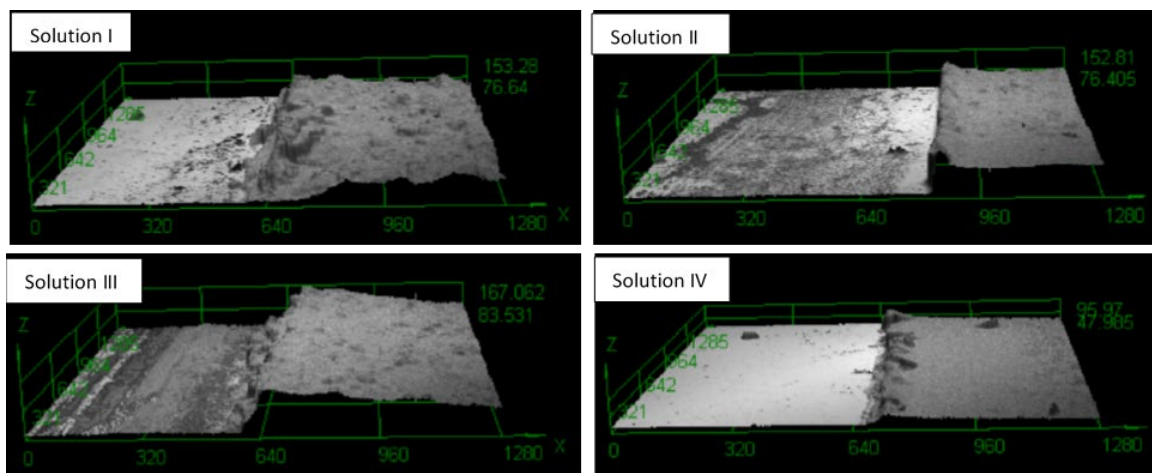


Fig. 6. 3D surface topography of TiO_2 coating at various TiO_2 solution

TiO_2 Coating Results at Various Plasma Irradiation Time. Using solution IV, the coating process was then conducted by varying plasma irradiation times of 0.5, 1, 2, 3, and 5 minutes. Roughness measurement record and roughness average are present in Figs. 7 and 8. The roughness average was increased as the plasma irradiation time. It was 3.39 μm , 4.37 μm , 4.06 μm , 5.12 μm , and 6.46 μm at plasma irradiation times of 0.5, 1, 2, 3, and 5 minutes, respectively. Figure 9 shows the thickness of the coating layer with a variation in plasma irradiation time. It was found to be 12.49 μm , 23.41 μm , 36.15 μm , 57.92 μm , and 77.55 μm at plasma irradiation times of 0.5, 1, 2, 3, and 5 minutes, respectively.

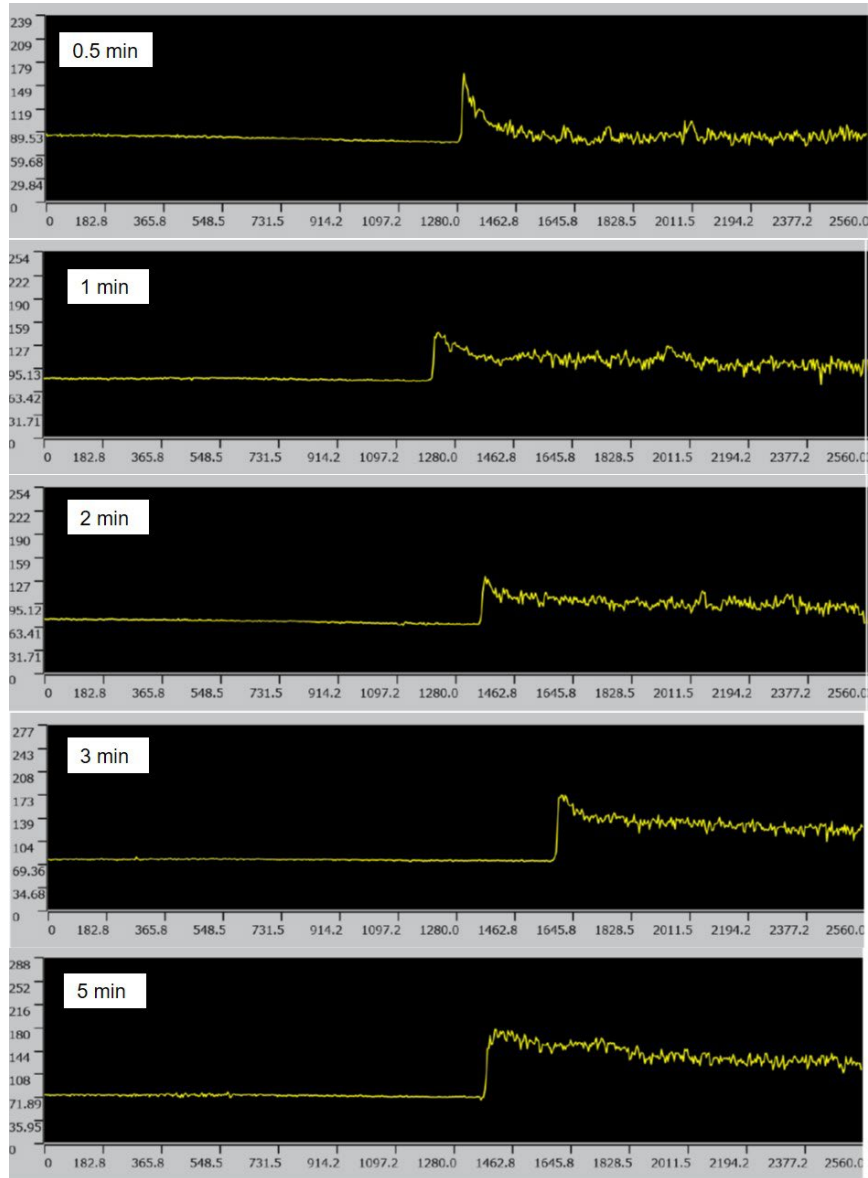


Fig. 7. Roughness measurement record of TiO₂ coating at various plasma irradiation times

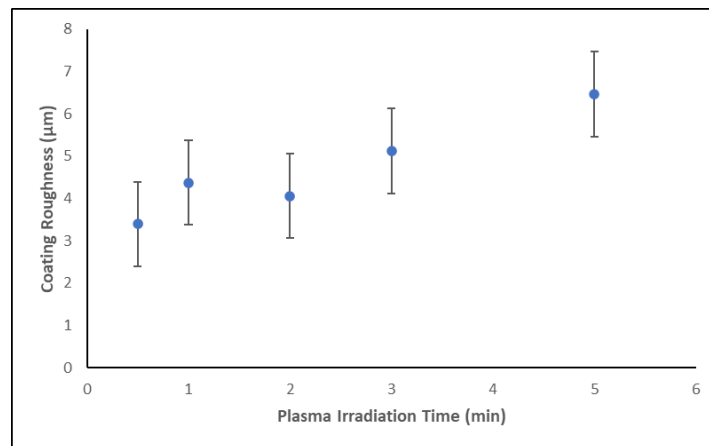


Fig. 8. Coating roughness average at various plasma irradiation time

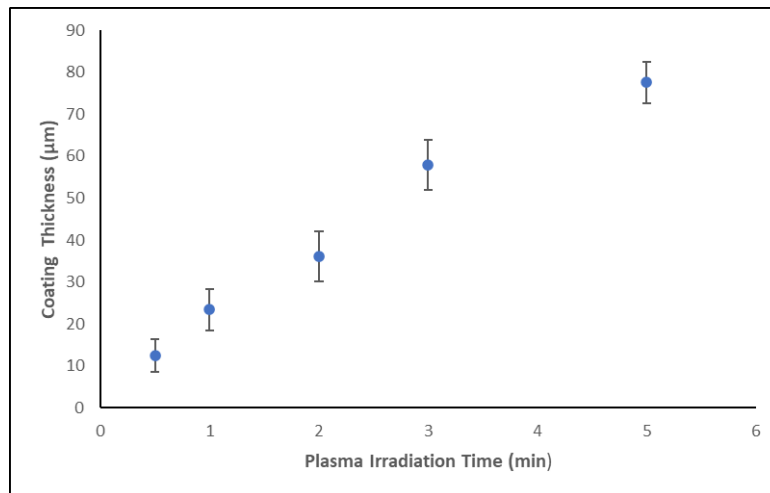


Fig. 9. Coating thickness average at various plasma irradiation time

Numerous papers deal with the influence of treatment time on roughness, thickness, and porosity. Research on the micro-arc oxidation coating method confirmed that as the oxidation time increase, the roughness and thickness constantly increase [27]. Increasing anodizing time of porous titania coating from 10 to 360 s resulting in a further increase of coating thickness, roughness, and porosity with 60 s of anodizing time is the most suitable for mechanically resistant titania coating [28].

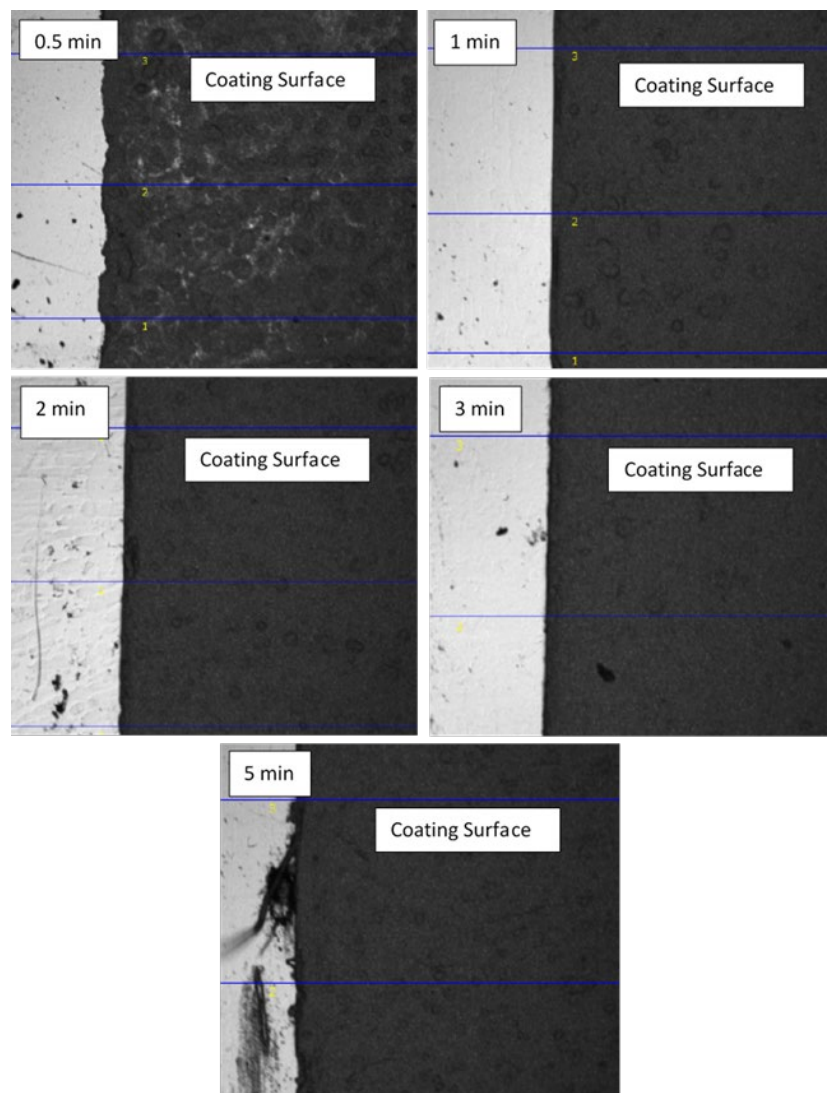


Fig. 10. Microstructure surface of TiO₂ coating at various plasma irradiation times

The thickness layer plays an important role in the efficiency of DSSC. Many studies have reported the optimum thickness for DSSC application. Research on TiO₂ deposited using the doctor blade method found that the best thickness ranged from 11 to 17 μm [29]. The single-layer TiO₂ photoanode deposited using the screen printing technique revealed that the average thickness of 12 μm can achieve the highest conversion efficiency of 5.13% [30]. Radio frequency (RF) plasma and Water Stabilized Plasma (WSP) methods reported that average coating thickness was obtained in a range of 0.47 to 3.02 μm [31]. In other work, several DSSCs were prepared with different semiconductor thicknesses to obtain the thickness-surface charge density dependence and it was found that the resistance of electrolyte solution was maximum at a thickness between 10 and 16 μm [32]. In this study, the optimum coating result was obtained when plasma was irradiated for 0.5 minutes with roughness and thickness of 3.398 μm and 12.499 μm respectively.

The morphology of the coating surface with a variety of plasma irradiation times is shown in figure 10. It was seen that the smaller pores obtained in 0.5 minute plasma irradiation time with an average size of 9.92 μm. In the plasma coating process, the TiO₂ solution was heated by plasma generation. A bubble containing plasma was touched and coated onto a conductive glass surface. Chemical reactions are initiated next, and then nucleation and growth of the grains occur, resulting in the formation of dense particles. Interactions among these highly active particles lead to the formation of either 'large' particles/crystals, agglomerates, or aggregates [33]. Another study reported that the plasma mechanism for coating formation occurred as the coating was shocked by bubble explosion due to the plasma heat [18].

Conclusion

As a preliminary investigation, the feasibility of TiO₂ coating on semiconductor conductive glass using the microwave plasma method has been conducted. An optimum coating result was obtained at a plasma generation time of 0.5 minutes with 12.49 μm and 3.398 μm of thickness and roughness respectively using 10 g TiO₂ + 50 ml ethanol and 40 ml H₂O. Further, the analysis will be conducted on the TiO₂ crystalline structure and coating mechanism of the microwave plasma method.

References

- [1] S. Umale, V. Sudhakar, S. M. Sontakke, K. Krishnamoorthy, and A. B. Pandit, Improved Efficiency of DSSC using Combustion Synthesized TiO₂, *Materials Research Bulletin*. 109 (2019) 222-226.
- [2] A. K. Baranwal *et al.*, Combining novel device architecture and NIR dye towards the fabrication of transparent conductive oxide-less tandem dye sensitized solar cell, *Applied Physics Express* 8 (2015) 1–3.
- [3] A. Hayat *et al.*, Dye-sensitized solar cells based on axially ligated phosphorus-phthalocyanine dyes, *Applied Physics Express* 8 (2015) 1–5.
- [4] N. A. Karim, U. Mehmood, H. F. Zahid, and T. Asif, Nanostructured photoanode and counter electrode materials for efficient Dye-Sensitized Solar Cells (DSSCs), *Solar Energy*. 185 (2019) 165–188.
- [5] J. Gong, J. Liang, and K. Sumathy, Review on dye-sensitized solar cells (DSSCs): Fundamental concepts and novel materials, *Renewable and Sustainable Energy Reviews*. 16 (2012) 5848–5860.
- [6] L. Nahar and I. U. Arachchige, Sol-Gel Methods for the Assembly of Metal and Semiconductor Nanoparticles, *JSM Nanotechnology and Nanomedicine*. 1 (2013) 1–6.
- [7] A. K. Krella, A. Krupa, M. Gazda, A. T. Sobczyk, and A. Jaworek, Protective properties of Al₂O₃ + TiO₂ coating produced by the electrostatic spray deposition method, *Ceramics International*. 43 (2017) 2126–2137.
- [8] W. Kim, J. Park, H. Kim, Y. Pak, H. Lee, and G. Y. Jung, Sequential Dip-spin Coating Method: Fully Infiltration of MAPbI₃-xCl_x into Mesoporous TiO₂ for Stable Hybrid Perovskite Solar Cells, *Electrochimica Acta*. 245 (2017) 734–741.

-
- [9] J. Sung, M. Shin, P. R. Deshmukh, H. S. Hyun, Y. Sohn, and W. G. Shin, Preparation of ultrathin TiO₂ coating on boron particles by thermal chemical vapor deposition and their oxidation-resistance performance, *Journal of Alloys and Compounds*. 767 (2018) 924–931.
- [10] N. Amaliyah, S. Mukasa, S. Nomura, and H. Toyota, Plasma In-liquid Method for Reduction of Zinc Oxide in Zinc Nanoparticle Synthesis, *Material Research Express*. 2 (2015).
- [11] Y. Hattori, S. Mukasa, H. Toyota, T. Inoue, and S. Nomura, Continuous synthesis of magnesium-hydroxide, zinc-oxide, and silver nanoparticles by microwave plasma in water, *Materials Chemistry and Physics*. 131 (2011) 425–430.
- [12] A. Ranjan, A. Islam, M. Pathak, M. K. Khan, and A. K. Keshri, Plasma sprayed copper coatings for improved surface and mechanical properties, *Vacuum*. 168 (2019) 108834.
- [13] G. Lin, J. Chen, W. Tseng, and F. Lu, Formation of Anatase TiO₂ coatings by plasma electrolytic oxidation for photocatalytic applications, *Surface & Coatings Technology*. 357 (2018).
- [14] H. Nagasawa, J. Xu, M. Kanezashi, and T. Tsuru, Atmospheric-pressure plasma-enhanced chemical vapor deposition of UV-shielding TiO₂ coatings on transparent plastics, *Materials Letters*. 228 (2018) 479–481.
- [15] A. Fattah-alhosseini, M. Molaei, and K. Babaei, The effects of nano- and micro-particles on properties of plasma electrolytic oxidation (PEO) coatings applied on titanium substrates: A review, *Surfaces and Interfaces*. 21 (2020) 100659.
- [16] Y. Bai, K. A. Kim, I. S. Park, S. J. Lee, T. S. Bae, and M. H. Lee, In situ composite coating of titania-hydroxyapatite on titanium substrate by micro-arc oxidation coupled with electrophoretic deposition processing, *Materials Science and Engineering B: Solid-State Materials for Advanced Technology*. 176 (2011) 1213–1221.
- [17] M. Aliofkhazraei, R. S. Gharabagh, M. Teimouri, M. Ahmadzadeh, G. B. Darband, and H. Hasannejad, Ceria embedded nanocomposite coating fabricated by plasma electrolytic oxidation on titanium, *Journal of Alloys and Compounds*. 685 (2016) 376–383.
- [18] E. Nikoomanzari, A. Fattah-alhosseini, M. R. Pajohi Alamoti, and M. K. Keshavarz, Effect of ZrO₂ nanoparticles addition to PEO coatings on Ti–6Al–4V substrate: Microstructural analysis, corrosion behavior and antibacterial effect of coatings in Hank's physiological solution, *Ceramics International*. 46 (2020) 13114–13124.
- [19] M. Roknian, A. Fattah-alhosseini, S. O. Gashti, and M. K. Keshavarz, Study of the effect of ZnO nanoparticles addition to PEO coatings on pure titanium substrate: Microstructural analysis, antibacterial effect and corrosion behavior of coatings in Ringer's physiological solution, *Journal of Alloys and Compounds*. 740 (2018) 330–345.
- [20] S. Sarbishei, M. A. Faghihi Sani, and M. R. Mohammadi, Effects of alumina nanoparticles concentration on microstructure and corrosion behavior of coatings formed on titanium substrate via PEO process, *Ceramics International*. 42 (2016) 8789–8797.
- [21] M. Shokouhfar and S. R. Allahkaram, Effect of incorporation of nanoparticles with different composition on wear and corrosion behavior of ceramic coatings developed on pure titanium by micro arc oxidation. 309 (2017).
- [22] P. Wang *et al.*, Effect of Al₂O₃ particle concentration on the characteristics of microarc oxidation coatings formed on pure titanium, *International Journal of Electrochemical Science*. 13 (2018) 8995–9006.
- [23] P. Wang *et al.*, Effect of MgO microparticles on characteristics of microarc oxidation coatings fabricated on pure titanium, *International Journal of Electrochemical Science*. 14 (2019) 287–300.
- [24] S. Di, Y. Guo, H. Lv, J. Yu, and Z. Li, Microstructure and properties of rare earth CeO₂-doped TiO₂ nanostructured composite coatings through micro-arc oxidation, *Ceramics International*. 41 (2015) 6178–6186.
- [25] A. Bordbar-Khiabani, S. Ebrahimi, and B. Yarmand, Highly corrosion protection properties of plasma electrolytic oxidized titanium using rGO nanosheets, *Applied Surface Science*. 486 (2019) 153–165.

- [26] H. Yu *et al.*, Surface & Coatings Technology Ti 3 AlC 2 coatings deposited by liquid plasma spraying, Surface & Coatings Technology. 299 (2016) 123–128.
- [27] L. Xu *et al.*, Effect of oxidation time on cytocompatibility of ultrafine-grained pure Ti in micro-arc oxidation treatment, Surface and Coatings Technology. 342 (2018) 12–22.
- [28] E. Santos *et al.*, Effect of anodizing time on the mechanical properties of porous titania coatings formed by micro-arc oxidation, Surface and Coatings Technology. 309 (2016) 203–211.
- [29] T. A. Ruhane *et al.*, Impact of photo electrode thickness and annealing temperature on natural dye sensitized solar cell, Sustainable Energy Technologies and Assessments. 20 (2017) 72–77.
- [30] A. Khalifa *et al.*, Comprehensive performance analysis of dye-sensitized solar cells using single layer TiO₂ photoanode deposited using screen printing technique, Optik. 223 (2020) 165595.
- [31] O. Kovářik *et al.*, The influence of substrate temperature on properties of APS and VPS W coatings, Surface and Coatings Technology. 268 (2015) 7–14.
- [32] D. Rangel, J. C. Gallegos, S. Vargas, F. García, and R. Rodríguez, Optimized dye-sensitized solar cells: A comparative study with different dyes, mordants and construction parameters,” Results in Physics. 12 (2018) 2026–2037.
- [33] J. Karthikeyan, C. C. Berndt, J. Tikkanen, S. Reddy, and H. Herman, Plasma spray synthesis of nanomaterial powders and deposits, Material Science & Engineering A. 238 (1997) 275–286.